Journal of Cultural Heritage 39 (2019) 13–20

Available online at
ScienceDirect
www.sciencedirect.com

Elsevier Masson France
EM|consulte
www.em-consulte.com/en

Original article

Absorption edge sensitive radiography and tomography of Egyptian Papyri☆

Tobias Arlt[a,*], Heinz-Eberhard Mahnke[b,c,d], Tzulia Siopi[b], Eve Menei[b,e], Cristina Aibéo[f], Regine-Ricarda Pausewein[f], Ina Reiche[f], Ingo Manke[d], Verena Lepper[b,g]

[a] Technische Universität Berlin, Germany
[b] Ägyptisches Museum und Papyrussammlung, Berlin, Germany
[c] Freie Universität Berlin, Germany
[d] Helmholtz-Zentrum Berlin, Germany
[e] Visiting conservator, 75002 Paris, France
[f] Rathgen-Forschungslabor SMB-SPK, Berlin, Germany
[g] Humboldt Universität zu Berlin, Germany

ARTICLE INFO

Article history:
Received 15 October 2018
Accepted 17 April 2019
Available online 7 May 2019

Keyword:
Elephantine papyri
Synchrotron absorption edge radiography
Non-destructive
X-ray
FT-IR
Lead carboxylate

ABSTRACT

In the Egyptian Museum and Papyrus Collection, Berlin, a multitude of papyrus manuscripts are stored. Papyri found on Elephantine island are of special interest. No other settlement in Egypt has been so well documented through texts over four millennia. However, 80% of the Elephantine texts are yet to be documented and published. As part of the "Elephantine" project, funded by an ERC starting grant, we attempt to gain access to hidden text. Most of the fragments are very fragile, deformed, with some rolled or folded. Papyri from the Old and Middle Kingdom were typically written with carbon ink. Consequently, these fragments show no absorption sensitivity for hard X-rays. Also, other inks have been used in those times. If small traces of high-Z elements, like Fe or Pb, are found, absorption may be sensitive enough for radiography and tomography to distinguish between writing and base material. We sorted out suitable fragments and papyrus packages by X-ray fluorescence mapping. When promising high-Z elements were detected, absorption tomography was applied using micro-CT laboratory systems or synchrotron X-rays at the BAMline at BESSY II. The sensitivity can be enhanced by element-sensitive absorption edge imaging, where transmission data taken above and below the edge are compared. This technique was applied at the absorption edges of the elements known to be used as ink and pigment material – Iron, Antimony and Lead. These X-ray results were complemented by Fourier-transform infrared spectroscopy (FT-IR) measurements showing that the lead is found in the form of lead carboxylate. In the future, the presented methodology will be applied to folded or rolled papyri, allowing for analysis of the text without manually opening the fragments.

1. Introduction

In the Egyptian Museum and Papyrus Collection Berlin a multitude of papyrus manuscripts is stored. Of special interest are papyri found on the island Elephantine.

The objective of the ERC research project ELEPHANTINE is to chronicle the 4000-year cultural history of Elephantine Island in Egypt. An important island in terms of military strategy, Elephantine is located in the Nile on Egypt's southern border as the center of the Aswan region. No other settlement in Egypt has been so well documented over such a long period. Its inhabitants comprised a multi-ethnic, multicultural and multi-religious community, which has left behind large amounts of written material, providing evidence of everyday life from the Old Kingdom right up to the era following the Arab conquest. The texts are written in various languages and scripts, including Hieroglyphs, Hieratic, Demotic, Aramaic, Greek, Coptic and Arabic [1,2,3]. In particular, carbon-based ink and metal ink [4], mainly containing iron, mercury, lead or copper, were used [5,6,7]. Especially copper is one element that has recently been discovered to be one ingredient for metal inks at an early stage of the ancient Egypt [8]. Eighty percent of the

☆ Paper selected from EMRS Spring Meeting 2018 SymposiumCC on Cultural Heritage.

* Corresponding author at: Technische Universität Berlin, Institut für Werkstoffwissenschaften, Strasse des 17. Juni 135, 10624 Berlin, Germany.
E-mail address: tobias.arlt@helmholtz-berlin.de (T. Arlt).

https://doi.org/10.1016/j.culher.2019.04.007
1296-2074/

Elephantine manuscripts are yet to be investigated and published [9]. Through international co-operation, the "papyrus puzzle" can thus be solved with the help of cutting-edge new methods from the digital humanities, physics or even mathematics and computer science. Most of the fragments are very fragile, small pieces, deformed, with some even rolled or folded. Therefore, it is impossible to gain access to the writing by manually opening some of these delicate and precious fragments. Here, we present a non-destructive and non-invasive technique based on X-ray imaging [10], allowing access to hidden text in rolled or folded manuscripts. FT-IR and Raman spectroscopy were also applied to obtain additional information about the chemical forms in which the detected elements were bound in the inks. Those methods are well established for analyzing fragile documents such as ancient papyri [11,12]. Especially synchrotron X-rays offer a variety of methods for cultural heritage [13].

2. Research aim

As part of the "Elephantine" project we try to gain access to hidden text. A non-destructive method, that allows access to hidden information, is urgently needed. Fortunately, the inter- and multidisciplinary research (e.g. imaging technology) has reached a high quality in recent years allowing this challenging problem to be addressed. We have developed a methodology that allows rapid access to hidden text. Potentially suitable fragments and papyrus packages are identified by X-ray fluorescence elemental mapping, using a portable instrument. Based on the XRF results, proper tomography techniques and setups are chosen, such as absorption or phase contrast tomography [14,15,16]. For convenience, micro CT laboratory systems containing a conventional vacuum X-ray tube can be used, but have limited spatial resolution and sensitivity to certain elements. Synchrotron devices, as used for the present work, are less available but allow for an energy selective tomography. Here, element-sensitive radiography was performed at the BAMline at BESSY II at Helmholtz-Zentrum Berlin, Germany.

The combination of these methods allows to select suitable samples, which are then subjected to more sensitive measurements. Although chemical compounds are an interesting topic and contain supplementary information. Here, we will only briefly discuss the issue of these compounds.

3. Material and methods

Information related to the Elephantine papyri that were selected for these measurements are described below.

3.1. Papyri fragments

Two fragments were analyzed in this study. Both fragments were taken from the Egyptian Museum Berlin and Papyrus Collection Berlin, Germany. Photographs of both the recto and the verso side are shown in Fig. 1. Fragment "ÄMP B/H × 133 g" (shown in Fig. 1a and b) contains two different writings in black and red ink on the recto side. The photograph of fragment "ÄMP B/H x 352" shows black ink, only. A tiny sample (<1 mm) was collected for FTIR analyses.

3.2. Portable XRF spectrometer

X-ray fluorescence (XRF) allows for a non-destructive elemental analysis of a sample. An incident beam of high energy X-rays is directed on to a sample. The emission from the sample, fluorescent X-rays, are detected by an energy-dispersive detector (8k MCA). An example is given in Fig. 2c, taken with the ELIO system

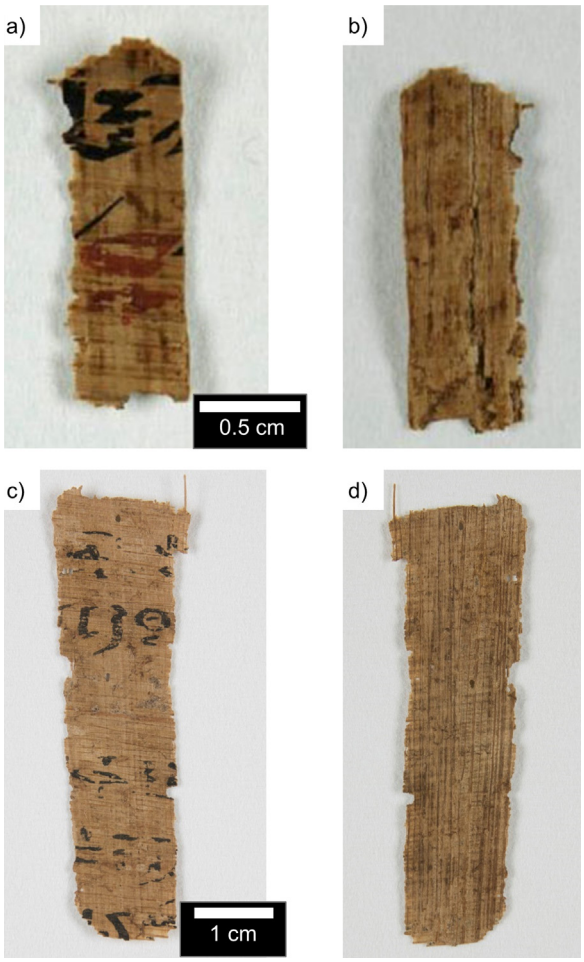

Fig. 1. a: Recto and b: verso side of fragment "ÄMP B/H × 133 g", c: recto and d: verso side of fragment "ÄMP B/H × 352". All photographs were taken by T. Siopi (ÄMP).

from XGLab [17]. For the presented measurements, a high voltage of 40 kV was applied to the Rh-anode of the X-ray tube, and a current of 200 μA was allowed. The incident X-ray beam was collimated to 1 mm^2. The setup is shown in Fig. 2a. The spot of the incoming X-ray beam is visualized by two laser points on the fragment, as seen in Fig. 2b. If both laser spots merge to one single spot, then the X-ray beam is focused on the surface of the fragment. Beside single point measurements, an element-sensitive mapping of whole fragments can be performed. For mapping, only a small energy bandwidth around an element-characteristic X-ray emission line is selected for each mapping point. The peak corresponds to one specific element. Subsequently, the scanning along the fragment's surface provides element-sensitive, two-dimensional information about the fragment.

3.3. Synchrotron imaging

Compared to laboratory X-ray devices, synchrotron X-rays exhibit a high brilliance. The most important consequences for imaging issues are the increased number of photons per unit of time and unit of cross-sectional area and a high degree of coherence. The latter is important for phase contrast measurements, whereas an increased number of photons allows for more and quicker energy-selective measurements within acceptable time periods. Essentially, this method may be considered to be non-destructive like conventional x-rays with the advantage of tailoring the useful energy of the synchrotron radiation needed for the investigation. However, in modern synchrotron facilities,

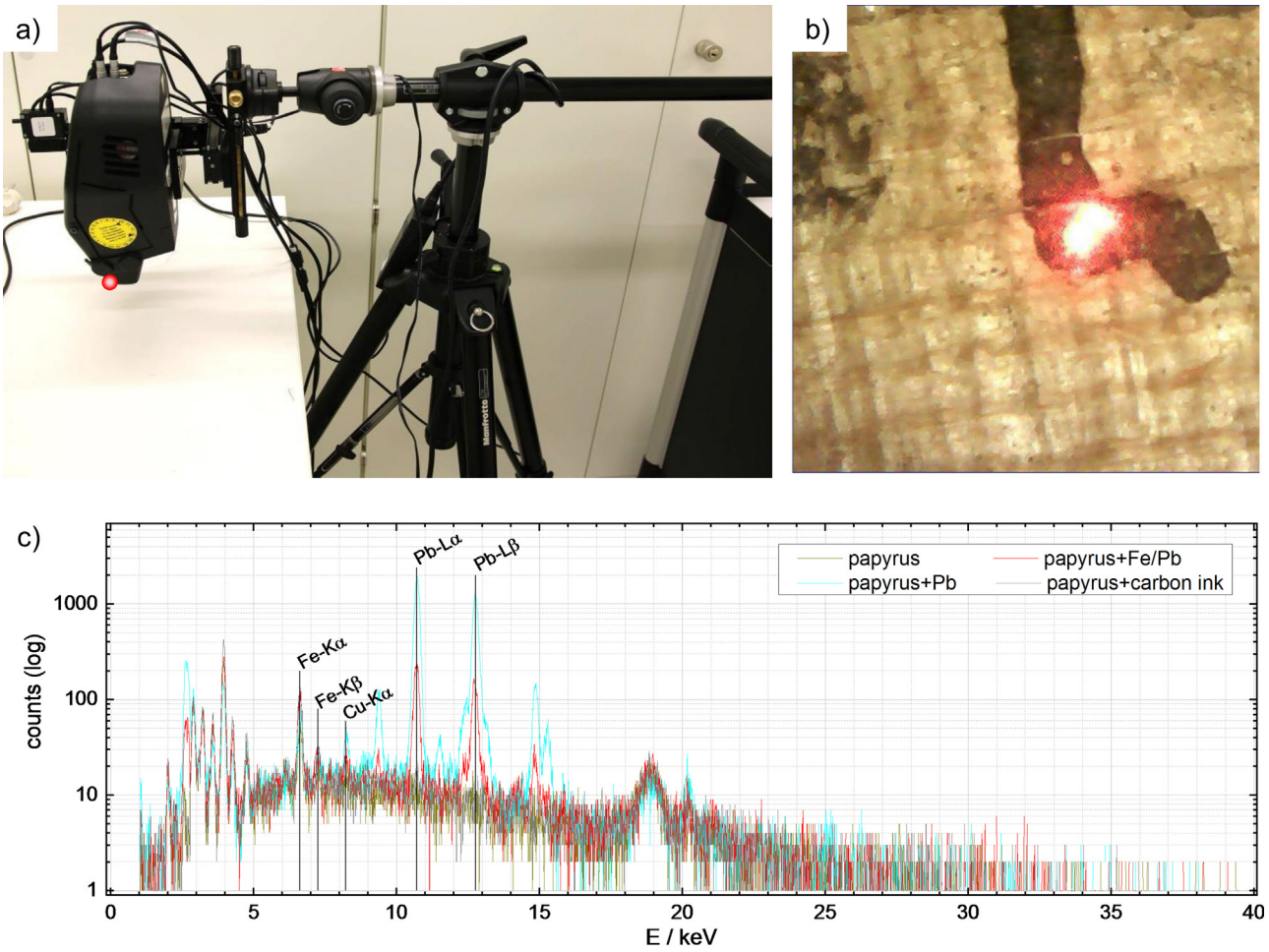

Fig. 2. a: Mobile XRF spectrometer ELIO, b: laser spot on fragment and c: measured spectra. For element-sensitive mapping, a proper energy bandwidth around one X-ray line (ṗeaḳ) was chosen.

so-called third generation and newer sources can easily deliver intensities much higher than typical X-ray tubes, so intensity tests are required before starting measurements

Hard X-ray synchrotron imaging was performed at the BAMline at the synchrotron source BESSY II at Helmholtz-Zentrum Berlin, Germany [18]. The electron storage ring was operated in top-up mode providing stable X-ray beam properties at the experimental stations. The tomography station at the BAMline allows for spatial analysis at high resolution for a multitude of samples. A sketch of the setup is shown in Fig. 3a. The required beam setup can be obtained using a system of different monochromators and slits. In this study a double multilayer monochromator (Si/W) was used in order to lower the energy bandwidth to $\Delta E/E = 10^{-2}$ (FWHM). An energy of 19 keV was chosen for standard radiographic measurements while 7.0 keV and 7.2 keV (Fig. 3b) and 12.90 keV and 13.15 keV were chosen for measurements at the absorption edges of Fe (K-edge) and of Pb (L_{23}-edge), respectively. With the versatile detector system, different magnification optics can be combined with different CCD cameras and scintillator screens. For the presented work, a 20-μm thick CWO_4 scintillator was combined with a 10-fold magnification optics and a pco4000 CCD camera, resulting in a pixel size of 440 nm.

The transmittance, which is the ratio of the incident beam I_0 and the transmitted beam I is measured with a spatial resolution of 440 nm for each pixel of the CCD camera. A scintillator converts X-rays to visible light, which is detected by the camera, see Fig. 3a. All radiograms were corrected for the camera offset and normalized to the beam intensity. The division of two radiograms, one taken below and the other one taken above the absorption edge, was done ex-situ. Consequently, the thickness of the specific element (here: Fe) can be calculated. The obtained images yield a higher sensitivity for thickness analysis than the transmission radiography. Element thicknesses of a few tens of nanometers can be determined. The normalization and image analysis were performed with ImageJ [19].

3.4. Raman spectroscopy

Raman spectroscopy is a proven method to investigate historical artifacts [20,21]. Here, it was done using the Horiba XploRa Raman-microscope equipped with Lasers at a wavelength of 532 nm, 638 nm, and 785 nm. By selecting different filters, microscope objectives and spectroscopic gratings, different beam intensities as well as spatial and spectroscopic resolutions can be achieved. The laser power was 25 mW (532 nm), 24 mW (638 nm) and 90 mW (785 nm). The maximum spatial resolution was 1 μm. The spectra are given in Raman shift [cm^{-1}] (shift of wavelength/frequency relative to the laser used given in wavenumbers). The calibration of the spectrum is accurate to approx. 2 cm^{-1}. Carbon could only be identified within the writings, see Fig. 4.

3.5. Fourier transform infrared spectroscopy

A Perkin Elmer instrument Paragon 1000 PC was used for the Fourier transform infrared spectroscopy, coupled with an FT-IR – microscope [22]. The spectrum was acquired in transmission mode

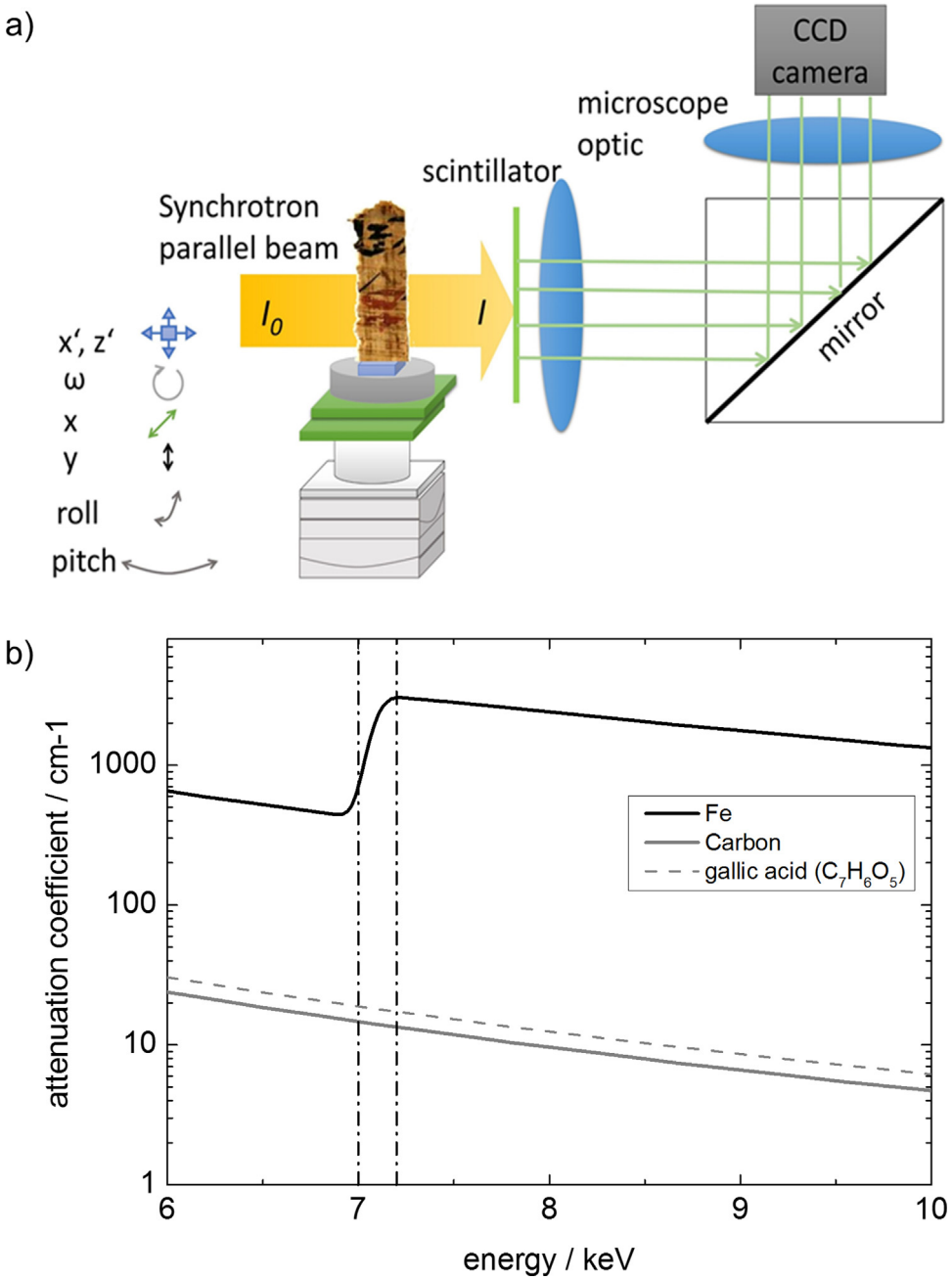

Fig. 3. a: Setup of X-ray radiography; b: Two discrete energies were selected below and above the absorption edge of the specific material (here: Fe); absorption coefficients taken from XOP software [3].

in the range of 4000–520 cm^{-1} with a resolution of 4 cm^{-1}. The sample was mounted on a diamond measuring cell from High Pressure Diamond Optics. The correlation of the spectroscopic data and the chemical data is shown in Table 1.

The preparation of Lead(II)stearate reference material was done on Dec 15, 1998 by C. Herm. 0.306 g (0.01 mol) sodium stearate ($C_{18}H_{37}O_2Na$) was dissolved in 10 mL water. Lead(II)acetate-trihydrate 0.190 g (0.05 mol) was added and the solution was subsequently brought to boiling point. A white precipitate was formed and filtered after cooling to room temperature. The residue was dried in ambient air. The yield was 0.390 g.

4. Results and discussion

A methodology that allows for element-selective measurements is presented in this work. It is focused on single-layered, flat fragments, since the method feasibility needs to be proven before applying it to 3d-objects.

As a first step, a mobile XRF spectrometer is used in order to obtain information about the content of metals inside the fragments. XRF is a fast accessible and easily available method. Although mapping allows for spatially resolved measurements, there are certain reasons to complement this method with others. One reason is the limited spatial resolution of portable XRF devices, often around a few mm^2 (in our case approximately $1 \times 1\ mm^2$ along the surface of the samples). This may be insufficient in order to detect legible writing. A more serious issue is related to the depth resolution perpendicular to the sample surface which ranges from rather limited to practically nonexistent. The penetration depth of the initial X-ray beam is quite high, but the emitted X-rays are of lower energy resulting in higher absorption from deeper parts of the sample. As such, the majority of the detected intensity contains

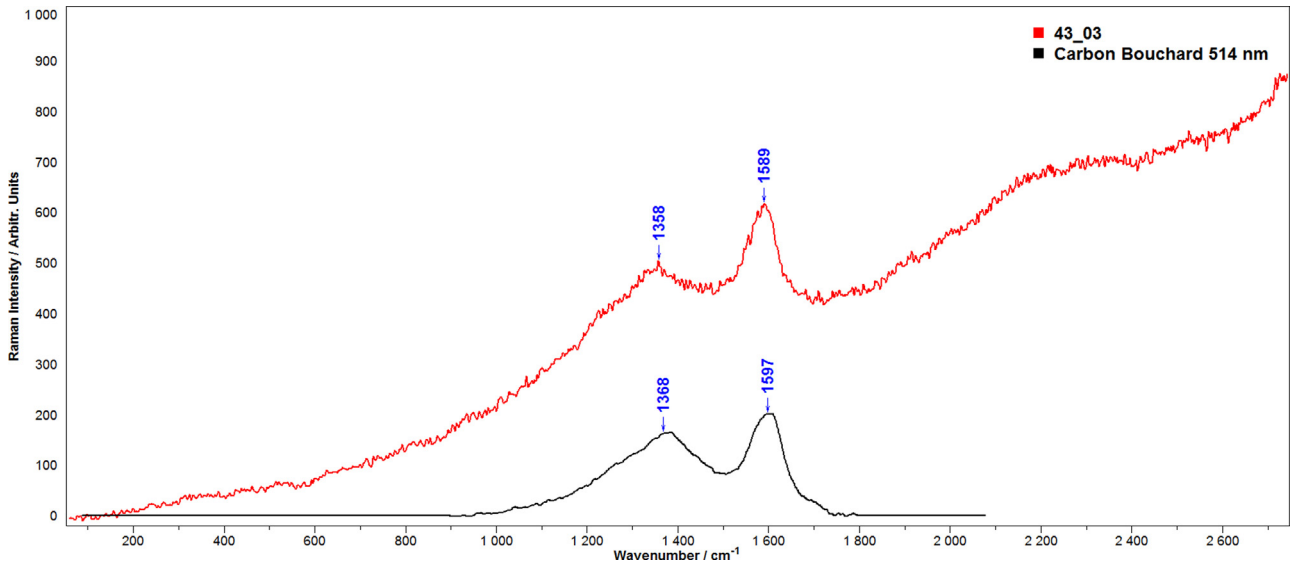

Fig. 4. Raman spectra of carbon reference (Carbon Bouchard at 514 nm, plotted in black) and of writing on fragment ÄMP B/H x 352 (plotted in red).

Table 1
Peak calibration of FT-IR spectra.

Wavenumber/cm^{-1}	Interpretation	Source
2919 + 2955sh	CH_2/CH_3 asymmetrical stretching	[26]
2850	CH_2/CH_3 symmetrical stretching	[26]
1512 + 1543 sh	COO- asymmetric stretching	[27]
1461	CH_2 bending (characteristic for lead palmitate or stearate	[27]
1419	COO- symmetric stretching	[27]
930	CH_2 rocking	[27]

near-surface information. Additionally the geometry for excitation and detection is optimized for the region where the X-ray beam hits the sample well focused. Consequently, this method can be considered as a surface-sensitive technique. Therefore, this (portable) XRF is very useful for getting initial, qualitative information about the sample.

For example, here we analyzed iron and lead. Iron was found in every papyrus fragment studied. This can be partly attributed to the manufacturing of the base material, the papyrus, as well as the origin, geological situation and the desert climate of the storage place, with an abundance of Fe containing materials like ochre or hematite found in most of the archeological sites. Thus, the iron content may also depend, to a varying degree, on the age of the fragments as well as on their former and intermediate storage containment and conditions. Additionally, the material of interest, the ink, contributes to the signal, too, if made out of ferrous ink. Therefore, qualitative information about the iron content and its areal distribution is of great interest. We also know that lead was used as a pigment, at least as an additive in inks in the Roman period, as well as occasional use prior to that. As such it is worth analysis.

The qualitative information, revealed by XRF, is a crucial criterion for selecting suitable fragments for time consuming tomography measurements.

The second step is X-ray transmission radiography. The ratio of the incident beam and the transmitted beam is detected spatially. The field of view is only $1.7 \times 1.2\,mm^2$ in width and height respectively. Therefore just a small part of the whole fragment was measured during these feasibility studies. Larger fragments or areas of interest must be scanned with a lower spatial resolution. Fig. 5a shows a photo of the fragment "ÄMP B/H × 133 g". Subfigure in 5b) gives an impression of the superimposed transmission radiogram. Areas of high X-ray attenuation (caused by ferrous particles or other high-Z elements) are shown in light gray values, areas of low attenuation are shown in dark gray values. The latter are attributed to low-Z elements like carbon. In this way, structures within the fragment and the group of high-Z elements can be identified two-dimensionally. The fiber structures of the papyri base material are clearly visible for the recto side (horizontal structure) and verso side (vertical structure) of the fragment. Additional bright spots can be observed, dispersed over the whole radiogram. These are probably metals, likely iron-containing dust. To verify this statement, a more detailed analysis is needed.

Consequently, as a third step, we applied synchrotron X-ray absorption edge radiography. This method is sensitive to single elements. A special element can be analyzed by selecting the corresponding energies closely below and above its absorption edge [23]. Energy edges with a sizable change of the attenuation, like K or L3 edges, are preferred. Thus the K-edge was chosen for iron, while the L3 edge was chosen for lead, since the K-edge of Pb (at 80 keV) is beyond the range of the beamline.

Fig. 5c-d show the results for fragment "ÄMP B/H × 133 g" for the absorption edge radiography for iron. Thicknesses of a few tens of nanometer can be analyzed. As indicated in Fig. 5c the absorbing effective Fe thickness is determined to be approximately 20 nm. The writing of the red ink, can also be identified in the X-ray images. The letter is emphasized in subfigure d). A direct comparison of transmission radiography and absorption edge radiography shows that the latter method is much more sensitive for the spatial distribution of the ink.

Compared to previous XRF measurements, the Fe distribution can be measured with a higher spatial resolution and now in a quantitative manner. First, the improvement allows for a more reliable letter recognition, which is barely possible with mobile XRF devices. The measurement of the total iron amount also may contribute to the letter recognition in multilayer fragments. Hereby, self-shielding becomes a rising problem for XRF measurements. Those measurements are planned for the future.

Another fragment "ÄMP B/H x 352" with hieratic writing was analyzed using absorption edge radiography. This fragment dates back to the Greco-Roman period. It is a single-layered, flat fragment and can mostly be read by the naked eye. Thus, it is well-suited for the testing of outstanding measuring methods. It is shown in Fig. 6. The easily visible writing had been written with carbon ink. No high-Z elements were found by XRF. Their meaning is "WLK" and does not provide any reliable information at this state of

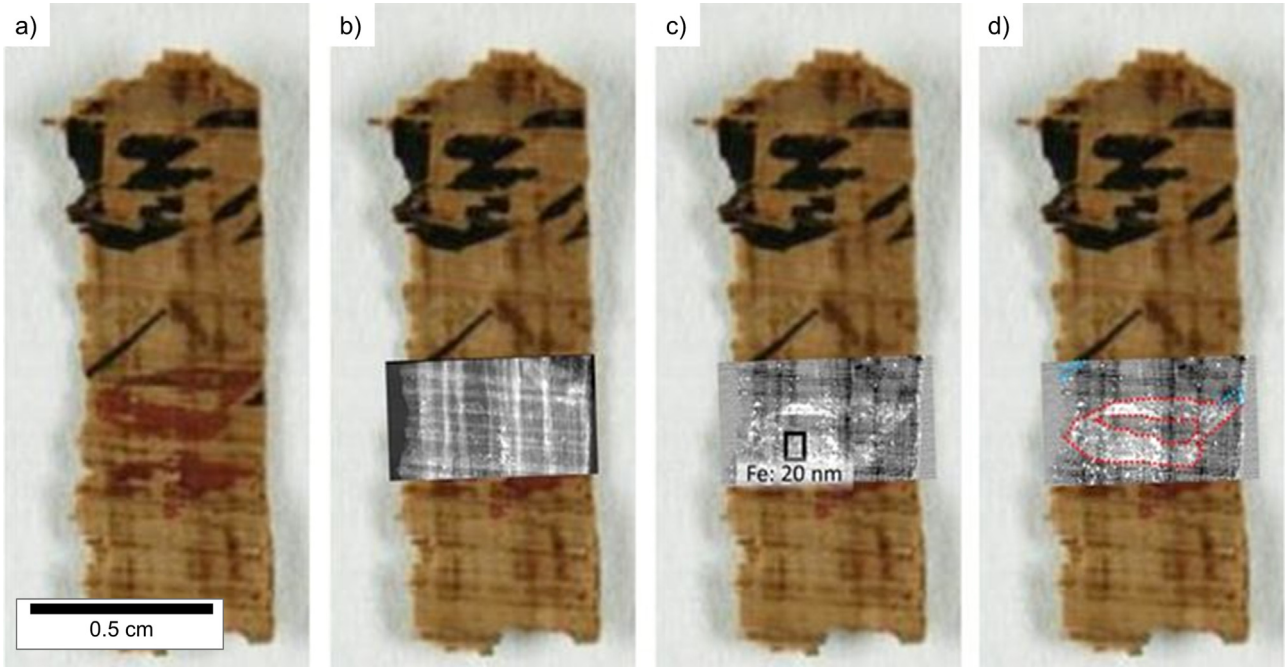

Fig. 5. Fragment "ÄMP B/H × 133 g". a: Photo of the fragment. Superimposed are in b: the transmission radiography, in c: the thickness of Fe, with the contours of the letter marked in red in d).

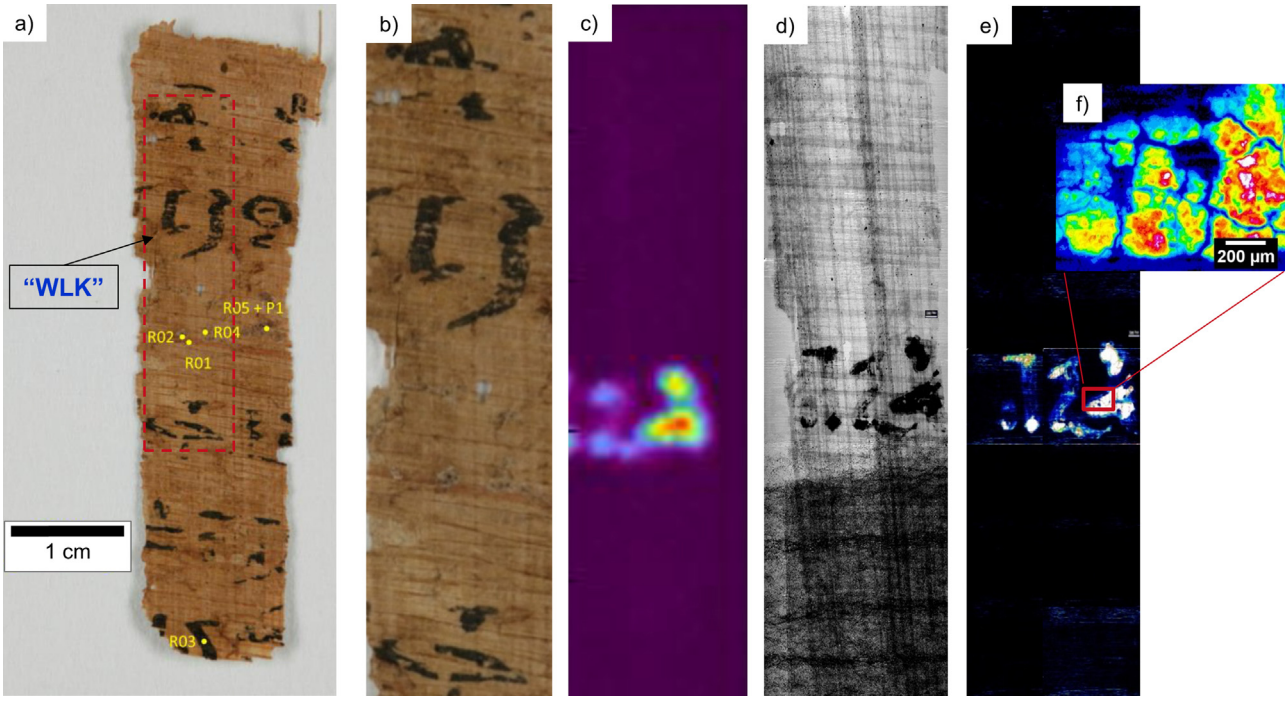

Fig. 6. Fragment "ÄMP B/H × 352"; a: Photo of the fragment with the area enlarged in b) marked and with indication of the Raman measurement's spots (R) and the sampling spot (P). Subfigures b)-e) show the same area. c) XRF mapping for Pb. d) Transmission radiography and e) absorption edge radiography at Pb_{L3} edge, with enlarged cutout.

knowledge. An enlargement of the fragment is shown in subfigure b). The same area was analyzed by lead-sensitive XRF mapping by filtering the Pb fluorescence spectrum around the Pb-L-line at 10.55 keV. The results are shown in subfigure c). Interestingly, a distinct signal was observed in areas without visible writing, and no signal where letters are visible, presumably written in carbon ink. A transmission radiogram taken at 19 keV is shown in d). Dark gray values represent elements with high atomic numbers. Consequently, there must be some elements with higher atomic number present. Switching the X-ray energy to the L3 absorption edge of lead revealed information that this attenuation is caused by lead, see subfigure e). An enlargement of the absorption edge measurement is shown in subfigure f). The thickness of lead is represented by false color. Cracks in the inks are visible. These are probably caused by the drying process over a long period of time. There was a possibility that the lead may be a mixed compound containing the element antimony. However, an absorption edge radiography at the K-edge of Sb gave no indication for the presence of antimony.

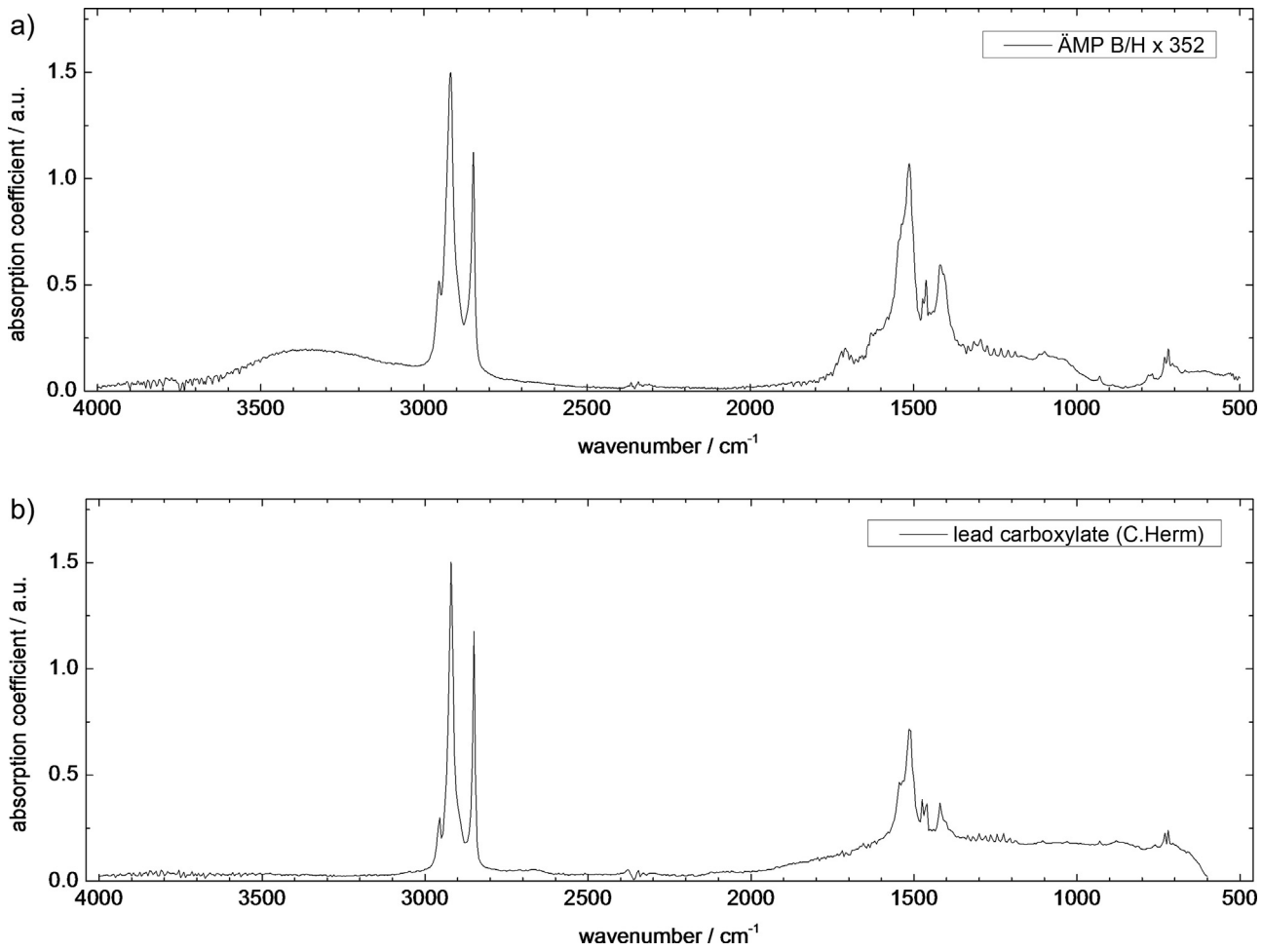

Fig. 7. a: FT-IR measurement within the area of the hidden symbol of fragment "ÄMP B/H × 352"; b: FT-IR of lead carboxylate (thanks to C. Herm for providing the reference sample and spectra).

Additionally, arsenic sulfide compounds like e.g. orpiment could also be present, as their existence could have escaped detection in the absorption edge radiography. However, the XRF spectra in the region of the hidden writing showed no significant contribution (see Fig. 2c).

The XRF on a single spot already showed a remarkable intensity in the Pb L-lines without any visible writing. That is a noticeably different to the findings reported by Christiansen [24] on various fragments of the Copenhagen collection, where the authors did not find any Pb in regions without writing (plain substrate). XRF and the presented absorption edge radiography only permit determination of the elements present in the ink material and enable the writing to become legible even when hidden, these methods do not give direct information on the chemical form in which the element is bonded. In step four we have therefore applied various infrared techniques sensitive to the chemical bonds.

We could confirm with Raman spectroscopy that carbon is the major component in the black ink (e.g. at the marked spot R03 in Fig. 6a), and hematite (spot R01) and goethite (spot R02) as typical components of red and yellow ochre. Nothing could be identified by means of Raman spectroscopy in the region of the intense lead and therefore a small piece was taken from this region (at R05 + P1) to be analyzed by means of FTIR.

Here, the Fourier transform infrared spectroscopy was employed on a small piece extracted from the aforementioned region (P1). The result is presented in Fig. 7, in comparison with a spectrum for lead carboxylate from the data base of the Rathgen-Forschungslabor, illustrating perfect agreement. This metal-organic compound is known to be invisible to optical light [25]. As such, it is not visible to the naked eye, but it does show up in FT-IR, and indirectly via the elemental sensitivity in absorption edge imaging. Consequently, the lead found in the fragment is due to the compound lead carboxylate. Its deliberate use as an ink for encryption seems very unlikely and, therefore, it is probably the result of a chemical transformation of a pigment that was originally used.

However, we can only speculate of what this pigment originally consisted. It could have been minium, the red mixed lead oxide Pb_3O_4, known to have been used in the Roman period, but also galena, black lead sulfide, or lead white, cannot be discounted. It is possible that the presence of carbon, oxygen and/or occasional moisture may have facilitated an optically stimulated transformation. Over such a long period of time, even slow process could potentially have led to complete reactions into non-colored compounds resulting in almost invisible writing.

Finally, it should be mentioned, although a translation is presently not possible, that the symbol revealed from the "hidden" text may be interpreted as a determinative for a divinity.

5. Conclusions and outlook

Cultural heritage research is an important, omnipresent, topic of human history. It offers great opportunities to look back on the past. However, it is essential to investigate historical artifacts in a non-destructive manner. This applies to the Elephantine Papyri. These fragments are extremely delicate, so that manual treatments

like unrolling or unfolding should be avoided. Nevertheless, getting access to the content of these fragments is of vital interest.

In the presented work, a promising combination of mobile XRF, synchrotron imaging and FT-IR was used in order to develop a methodology that allows visualizing ink in ancient papyri. With the advantage of being able to verify the results by visual inspection, two-dimensional papyri were examined in this feasibility study. The focus was on papyri that were written with ferrous or plumbiferous ink.

While XRF mapping turned out to be a straightforward method that allows for a rough location of iron inside a fragment, the spatial information and the sensitivity of the mobile XRF spectrometer may not be sufficient to make the writing legible. Transmission radiography provides an improved spatial resolution. When inks containing high-Z elements have a sufficient thickness, an extraction of the textual information is possible. As demonstrated, absorption edge imaging improves the sensitivity to specific elements with a very effective background suppression. By choosing well-defined energies around the absorption edge of the element in question, it delivers very detailed information about the distribution and thickness of this specific element. In the presented work, this is shown for ferrous and plumbiferous ink, but is applicable to other elements as well, provided the energy of the X-ray beam can easily be varied, as is the case at most synchrotron sources.

Here, the combination of the above mentioned methods yielded interesting results which were complemented by FT-IR measurements: lead was found in areas without any visible ink, and the chemical compound was identified as lead carboxylate. This is remarkable, since our example presents evidence for the use of a lead compound as ink material, not just as an additive, during this historical period.

As a next step, these methods will be applied to folded or rolled fragments. Even for 3D analysis, the spatial and temporal resolution of the presented methods seem to be well suited. The only crucial issue is the availability of suitable synchrotron beamlines.

Funding

This work was funded by the European Research Council (ERC) project ELEPHANTINE “Localizing 4000 Years of Cultural History. Texts and Scripts from Elephantine Island in Egypt” [Project ID 637692, funded under H2020-EU.1.1.].

Disclosure of interest

The authors declare that they have no competing interest.

Acknowledgments

The authors gratefully acknowledge Dr. Robert Bradbury from Technical University Berlin for proof reading and constructive criticism of the manuscript.

References

[1] P.T. Nicholson, I. Shaw, Ancient Egyptian Materials and Technology, Cambridge University Press, 2009 (ISBN 978-0521120982).
[2] D.A. Scott, A review of ancient Egyptian pigments and cosmetics, Stud. Conserv. 61 (4) (2016) 185–202, http://dx.doi.org/10.1179/2047058414Y.0000000162.
[3] D.B. Gore, M. Choat, D.E. Jacob, G. Gloy, Which elements are useful for understanding the composition of ancient papyrus inks? Powder Diffraction 32 (Supplement S2) (2017) S90–S94, http://dx.doi.org/10.1017/S0885715617000951.
[4] B. Wagner, M.L. Donten, M. Donten, E. Bulska, A. Jackowska, W. Sobucki, Analytical approach to the conservation of the ancient Egyptian manuscript ‘Bakai Book of the Dead’: a case study, Mikrochim Acta 159 (2007) 101–108, http://dx.doi.org/10.1007/s00604-007-0732-0.
[5] C. Graux, L’encre à base métallique dans l’antiquité, Rev. Philolol. IV (1880) 82–85.
[6] E. Brun, M. Cotte, J. Wright, M. Ruat, P. Tack, L. Vincze, C. Ferrero, D. Delattre, V. Mocella, Revealing metallic ink in Herculaneum papyri, PNAS 113 (14) (2016) 3751–3754, http://dx.doi.org/10.1073/pnas.1519958113.
[7] M. Uda, Characterization of Pigments Used in Ancient Egypt, in: M. Uda, G. Demortier, I. Nakai (Eds.), X-rays for Archaeology, Springer, Dordrecht, 2005, http://dx.doi.org/10.1007/1-4020-3581-0_1 (Print ISBN 978-1-4020-3580-7, Online ISBN 978-1-4020-3581-4).
[8] T. Christiansen, M. Cotte, R. Loredo-Portales, P.E. Lindelof, K. Mortensen, K. Ryholt, S. Larsen, The nature of ancient Egyptian copper-containing carbon inks is revealed by synchrotron radiation based X-ray microscopy, Sci. Rep. 7 (2017) 15346, http://dx.doi.org/10.1038/s41598-017-15652-7.
[9] R. Enmarch, V.M. Lepper, Ancient Egyptian Literature: Theory and Practice, Oxford University Press, Proceedings of the British Academy 188 (2013), http://dx.doi.org/10.5871/bacad/9780197265420.001.0001 (289 pp).
[10] I. Bukreeva, G. Ranocchia, V. Formoso, M. Alessandrelli, M. Fratini, L. Massimi, A. Cedola, Chapter 13 - Investigation of Herculaneum Papyri by X-Ray Phase-Contrast Tomography, Nanotechnologies and Nanomaterials for Diagnostic, Conservation and Restoration of Cultural Heritage, Adv. Nanomaterials (2019) 299–324, http://dx.doi.org/10.1016/B978-0-12-813910-3.00013-6.
[11] F. Cappa, B. Fruehmann, M. Schreiner, Chapter 7 - Raman Spectroscopy for the Material Analysis of Medieval Manuscripts, Nanotechnologies and Nanomaterials for Diagnostic, Conservation and Restoration of Cultural Heritage, Adv. Nanomaterials (2019) 127–147, http://dx.doi.org/10.1016/B978-0-12-813910-3.00007-0.
[12] S. Mosca, T. Frizzi, M. Pontone, R. Alberti, L. Bombelli, V. Capogrosso, A. Nevin, G. Valentini, D. Comelli, Identification of pigments in different layers of illuminated manuscripts by X-ray fluorescence mapping and Raman spectroscopy, Microchem. J. (2016) 775–784, http://dx.doi.org/10.1016/j.microc.2015.10.038.
[13] M. Cotte, A. Genty-Vincent, K. Janssens, J. Susini, Applications of synchrotron X-ray nano-probes in the field of cultural heritage, C. R. Phys. 19 (7) (2018) 575–588, http://dx.doi.org/10.1016/j.crhy.2018.07.002.
[14] V. Mocella, E. Brun, C. Ferrero, D. Delattre, Revealing letters in rolled Herculaneum papyri by X-ray phase-contrast imaging, Nat. Commun. 6 (2015) 5895, http://dx.doi.org/10.1038/ncomms6895.
[15] T. Arlt, I. Manke, K. Wippermann, C. Tötzke, H. Markötter, H. Riesemeier, J. Mergel, J. Banhart, Investigation of the three-dimensional ruthenium distribution in fresh and aged membrane electrode assemblies with synchrotron X-ray absorption edge tomography, Electrochemistry Commun. 13 (8) (2011) 826–829, http://dx.doi.org/10.1016/j.elecom.2011.05.013.
[16] J. Banhart, Advanced Tomographic Methods in Materials Research and Engineering, Oxford Scholarship Online, Oxford, 2008, http://dx.doi.org/10.1093/acprof:oso/9780199213245.001.0001 (ISBN 9780199213245).
[17] https://www.bruker.com/products/x-ray-diffraction-and-elemental-analysis/micro-xrf-and-txrf/elio/technical-details.html, (last access: April 12, 2019).
[18] W. Görner, M.P. Hentschel, B.R. Müller, H. Riesemeier, M. Krumrey, G. Ulm, W. Diete, U. Klein, R. Frahm, BAMline: the first hard X-ray beamline at BESSY II, Nuclear Instruments and Methods in Physics Research Section A: accelerators, Spectrometers, Detectors and Associated Equipment 467-468 (2001) 703–706, http://dx.doi.org/10.1016/S0168-9002(01)00466-1.
[19] C.A. Schneider, W.S. Rasband, K.W. Eliceiri, NIH Image to ImageJ: 25 years of image analysis, Nat. Methods 9 (7) (2012) 671–675 https://www.ncbi.nlm.nih.gov/pmc/articles/PMC5554542/.
[20] A.R. David, H.G.M. Edwards, D.W. Farwell, D.L.A. De Faria, Raman Spectroscopic Analysis of Ancient Egyptian Pigments, Archaeometry 43 (4) (2001) 461–473, http://dx.doi.org/10.1111/1475-4754.00029.
[21] J. Ambers, Raman analysis of pigments from the Egyptian Old Kingdom, Journal of Raman Spectroscopy, 35(8-9), Special Issue: Raman spectroscopy in Art and Archaeology (2004) 768–773, http://dx.doi.org/10.1002/jrs.1187.
[22] J. Łojewska, I. Rabin, D. Pawcenis, J. Bagniuk, M.A. Aksamit-Koperska, M. Sitarz, M. Missori, M. Krutzsch, Recognizing ancient papyri by a combination of spectroscopic, diffractional and chromatographic analytical tools, Sci. Rep. 7 (2017) 46236, http://dx.doi.org/10.1038/srep46236.
[23] T. Arlt, I. Manke, K. Wippermann, H. Riesemeier, J. Mergel, J. Banhart, Investigation of the local catalyst distribution in an aged direct methanol fuel cell MEA by means of differential synchrotron X-ray absorption edge imaging with high energy resolution, J. Power Sources 221 (2013) 210–216, http://dx.doi.org/10.1016/j.jpowsour.2012.08.038.
[24] T. Christiansen, D. Buti, K.N. Dalby, P.E. Lindelof, K. Ryholt, A. Vila, Chemical characterization of black and red inks inscribed on ancient Egyptian papyri: The Tebtunis temple library, J. Archaeol. Sci. Rep. 14 (2017) 208–219, http://dx.doi.org/10.1016/j.jasrep.2017.05.042.
[25] C. Zhang, B. Wang, W. Li, S. Huang, L. Kong, Z. Li, L. Li, Conversion of invisible metal-organic frameworks to luminescent perovskite nanocrystals for confidential information encryption and decryption, Nat. Commun. 8 (2017) 1138, http://dx.doi.org/10.1038/s41467-017-01248-2.
[26] G. Socrates, Infrared and Raman Charecteristic Group Frequencies: Tables and Charts, 3rd Ed., John Wiley & Sons, LTD, Chichester, 2004 (ISBN: 978-0-470-09307-8).
[27] Otero, et al., Characterisation of metal carboxylates by Raman and infrared spectroscopy in works of art, J. Raman Spectrosc. 45 (11-12) (2014) 1197–1206, http://dx.doi.org/10.1002/jrs.4520 (Special Issue: Raman in Art and Archaeology 2013).